Numer. Math. (2017) 135:1–26
DOI 10.1007/s00211-016-0799-9

Numerische Mathematik

Approximation of functions of large matrices with Kronecker structure

Michele Benzi[1] · **Valeria Simoncini**[2,3]

Received: 8 March 2015 / Revised: 9 February 2016 / Published online: 22 March 2016

Abstract We consider the numerical approximation of $f(\mathcal{A})b$ where $b \in \mathbb{R}^N$ and $\mathcal{A}$ is the sum of Kronecker products, that is $\mathcal{A} = M_2 \otimes I + I \otimes M_1 \in \mathbb{R}^{N \times N}$. Here f is a regular function such that $f(\mathcal{A})$ is well defined. We derive a computational strategy that significantly lowers the memory requirements and computational efforts of the standard approximations, with special emphasis on the exponential and on completely monotonic functions, for which the new procedure becomes particularly advantageous. Our findings are illustrated by numerical experiments with typical functions used in applications.

Mathematics Subject Classification 65F60

The work of M. Benzi was supported by National Science Foundation Grants DMS-1115692 and DMS-1418889. The work of V. Simoncini was partially supported by the FARB12SIMO Grant of the Università di Bologna.

✉ Michele Benzi
benzi@mathcs.emory.edu

Valeria Simoncini
valeria.simoncini@unibo.it

1 Department of Mathematics and Computer Science, Emory University, Atlanta, Georgia 30322, USA

2 Dipartimento di Matematica, Università di Bologna, Piazza di Porta S. Donato 5, 40127 Bologna, Italy

3 IMATI-CNR, Pavia, Italy

1 Introduction

We consider the problem of approximating

$$f(\mathcal{A})b \tag{1.1}$$

where f is a sufficiently regular function defined on the spectrum of $\mathcal{A}$ (see [25]), and

$$\mathcal{A} = M_1 \oplus M_2 := M_2 \otimes I + I \otimes M_1 \in \mathbb{R}^{N\times N} \tag{1.2}$$

is the sum of Kronecker products with $M_1 \in \mathbb{R}^{n_1\times n_1}$, $M_2 \in \mathbb{R}^{n_2\times n_2}$ so that $N = n_1 n_2$, $b = \mathrm{vec}(B)$ with B a matrix of low rank with dimensions compatible with that of b. The Kronecker (or tensor) product of two matrices X and Y of size $n_x \times m_x$ and $n_y \times m_y$, respectively, is defined as

$$X \otimes Y = \begin{bmatrix} x_{11}Y & x_{12}Y & \cdots & x_{1m_x}Y \\ x_{21}Y & x_{22}Y & \cdots & x_{2m_x}Y \\ \vdots & \vdots & \ddots & \vdots \\ x_{n_x1}Y & x_{n_x2}Y & \cdots & x_{n_xm_x}Y \end{bmatrix} \in \mathbb{R}^{n_xn_y\times m_xm_y};$$

the vec operator stacks the columns of a matrix $X = [x_1, \ldots, x_m] \in \mathbb{R}^{n\times m}$ one after the other as

$$\mathrm{vec}(X) = \begin{bmatrix} x_1 \\ \vdots \\ x_m \end{bmatrix} \in \mathbb{R}^{nm\times 1}.$$

The problem of approximating (1.1) for general $\mathcal{A}$ is very important in several applications and has long attracted considerable attention; we refer the reader to [25] and to [35] for comprehensive treatments of the problem and for many ways of numerically approximating its solution. For the case when $\mathcal{A}$ has large dimensions, new effective approaches have been devised, making the use of matrix function evaluations an important tool for solving large scale (three-dimensional) scientific and engineering problems involving discretized partial differential equations; see, e.g., [15,27,28], where the exponential and the related φ-functions are employed. Other functions of interest in certain discretizations of elliptic or evolutionary problems include $\exp(z)$, $z^{-1/2}$, $\exp(-a\sqrt{z})$ and their rational function combinations; see, e.g., [8,10] and references therein. The Kronecker structure above arises whenever the domain is a rectangle or a parallelepiped and finite difference, isogeometric or certain low-order finite element methods on tensor product grids are employed to discretize differential equations with separable coefficients; see, e.g., [37] and references therein. Low rank matrices B such that $b = \mathrm{vec}(B)$ naturally arise in parabolic PDEs when the initial data is low rank, or in elliptic problems when certain classes of boundary conditions are imposed. In the latter applications, although the possibly smooth source terms rarely show a low rank structure, they can often be approximated by matrices

with the desired low rank form; see also the discussion in [4]. Other applications leading to matrices with Kronecker sum structure include image processing [24], queueing theory [36, Chapter 9], graph analysis [1, Chapter 3.4], and network design [42].

A significant body of literature is now available on efficient numerical methods for approximately evaluating the product of $f(\mathcal{A})$ times a vector b, using particular spectral properties of $\mathcal{A}$ and under certain regularity conditions on f. Also, there are several papers in which the Kronecker structure of $\mathcal{A}$ is exploited to construct fast algorithms for the evaluation of $f(\mathcal{A})b$ using integral representations of f and numerical quadrature together with $\mathscr{H}$-matrix techniques; see, e.g., [16,17,19,21,22]. To the best of our knowledge, however, the computational advantages of exploiting, for a general function f, the possible Kronecker structure of $\mathcal{A}$ have not been addressed in the context of Krylov subspace methods for large-scale problems of the form (1.1). By taking into account this structure, and also the possible low rank of B, the computational setting changes significantly. We will show that by preserving the structure of the problem, faster convergence and significantly lower memory requirements can be achieved. More precisely, we acknowledge that the approximation to functions of $\mathcal{A}$ is the composition of distinct approximations in terms of M_1 and M_2, which are much smaller matrices. Similar considerations can be made for other properties of functions of matrices that are Kronecker sums, as is the case for their sparsity and decay patterns; see [7] for a recent analysis.

Our results strongly rely on the low rank of the matrix B. In fact, but without loss of generality, we shall assume that B has rank equal to one, so that we can write $B = b_1 b_2^T$, $b_1 \in \mathbb{R}^{n_1}$, $b_2 \in \mathbb{R}^{n_2}$. For larger rank $\ell \ll \min\{n_1, n_2\}$, we could still write $B = B_1 B_2^T$ and proceed in a similar manner. Our results also apply when B is *numerically* low rank, that is, only a few singular values of B are above machine precision, or some other small tolerance. In this case, we could write $b = \widehat{b} + b_\epsilon$ where $\widehat{b} = \mathrm{vec}(\widehat{B})$ with $\widehat{B}$ of low rank, and $\|b_\epsilon\| \ll 1$. If $\|f(\mathcal{A})\|$ is not too large,

$$f(\mathcal{A})b = f(\mathcal{A})\widehat{b} + f(\mathcal{A})b_\epsilon \approx f(\mathcal{A})\widehat{b}.$$

An outline of the paper is as follows. In Sect. 2 we review some standard techniques for approximating (1.1) when $\mathcal{A}$ is large, and set up the notation for the rest of the paper. In Sect. 3 we derive the structure-exploiting approximation for general functions f such that $f(\mathcal{A})$ is well defined. In Sect. 4 we focus on the exponential function, for which the new procedure becomes particularly advantageous. Another important special case, the matrix inverse, is briefly discussed in Sect. 5, and more general matrix functions in Sect. 6. Conclusions are given in Sect. 7. Our findings are illustrated by numerical experiments with typical functions used in applications.

2 General approximation by projection

A common procedure for large $\mathcal{A}$ constructs an approximation space, and a matrix $\mathcal{V}$ whose orthonormal columns span that space, and obtain

$$f(\mathcal{A})b \approx \mathcal{V} f(H) e, \qquad H = \mathcal{V}^T \mathcal{A} \mathcal{V}, \quad e = \mathcal{V}^T b. \tag{2.1}$$

Depending on the spectral properties of the matrix $\mathcal{A}$ and on the vector b, the approximation space dimension may need to be very large to obtain a good approximation. Unfortunately, the whole matrix $\mathcal{V}$ may need to be stored, limiting the applicability of the approach. This is the motivation behind the recently introduced restarted methods, which try to cope with the growing space dimensions by restarting the approximation process as soon as a fixed maximum subspace dimension is reached [11,14]. In the symmetric case, another approach could be a so-called two-pass strategy, where the orthonormal basis is first built to generate H but not stored; after having computed $y = f(H)e$, it is built again to obtain the product $\mathcal{V}y$.

A classical choice as approximation space is given by the (standard) Krylov subspace[1] $K_m(\mathcal{A}, b) = \text{span}\{b, \mathcal{A}b, \ldots, \mathcal{A}^{m-1}b\}$. An orthonormal basis $\{v_1, \ldots, v_m\}$ can be constructed sequentially via the Arnoldi recurrence, which can be written in short as

$$\mathcal{A}\mathcal{V}_m = \mathcal{V}_m H_m + h v_{m+1} e_m^T, \qquad \mathcal{V}_m = [v_1, \ldots, v_m];$$

here e_m is the mth vector of the canonical basis of $\mathbb{R}^m$, $H_m = \mathcal{V}_m^T \mathcal{A} \mathcal{V}_m$ (as stated earlier), and $h = \|\mathcal{A}v_m - \sum_{i=1}^m [H_m]_{im} v_i\|$.

The past few years have seen a rapid increase in the use of richer approximation spaces than standard Krylov subspaces. More precisely, rational Krylov subspaces, namely

$$\mathbb{K}_m(\mathcal{A}, b, \boldsymbol{\sigma}_{m-1}) = \text{span}\{b, (\mathcal{A} - \sigma_1 I)^{-1} b, \ldots, \prod_{i=1}^{m-1} (\mathcal{A} - \sigma_i I)^{-1} b\}, \qquad (2.2)$$

have been shown to be particularly well suited for matrix function approximations; we refer the reader to [20] for a recent survey on various issues related to rational Krylov subspace approximations of matrix functions. A special case is given by the extended Krylov subspace, which alternates powers of $\mathcal{A}$ with powers of $\mathcal{A}^{-1}$ [8,31].

3 Exploiting the Kronecker structure

Assume that $\mathcal{A}$ has the form in (1.2) and that, for simplicity, B has rank one, that is $B = b_1 b_2^T$. We generate distinct approximations for the matrices M_1 and M_2; in the case of the classical Krylov subspace these are given as

$$K_m(M_1, b_1), \quad M_1 Q_m = Q_m T_1 + q_{m+1} t^{(1)} e_m^T$$

and

$$K_m(M_2, b_2), \quad M_2 P_m = P_m T_2 + p_{m+1} t^{(2)} e_m^T.$$

Note that the two spaces could have different dimensions; we will use the same dimension for simplicity of presentation. The matrices Q_m and P_m have orthonor-

[1] In case b is a matrix, the definition of a "block" Krylov subspace is completely analogous, that is $K_m(\mathcal{A}, b) = \text{range}([b, \mathcal{A}b, \ldots, \mathcal{A}^{m-1}b])$.

mal columns, and have a much smaller number of rows than $\mathcal{V}_m$ (the square root of it, if $n_1 = n_2$). We thus consider the following quantity to define the approximation:

$$\mathcal{V} = P_m \otimes Q_m$$

so that

$$\begin{aligned}\mathcal{A}\mathcal{V} &= \mathcal{A}(P_m \otimes Q_m) = M_2 P_m \otimes Q_m + P_m \otimes M_1 Q_m \\ &= (P_m T_2 \otimes Q_m + P_m \otimes Q_m T_1) + p_{m+1} t^{(2)} e_m^T \otimes Q_m + P_m \otimes q_{m+1} t^{(1)} e_m^T \\ &= (P_m \otimes Q_m)(T_2 \otimes I_m + I_m \otimes T_1) + \text{low rank}.\end{aligned}$$

Following the general setting in (2.1), and defining $\mathcal{T}_m = T_2 \otimes I_m + I_m \otimes T_1$ we thus consider the approximation

$$f(\mathcal{A})b \;\approx\; x_m^{\otimes} := (P_m \otimes Q_m)z, \quad z = f(\mathcal{T}_m)(P_m \otimes Q_m)^T b. \tag{3.1}$$

We stress that the matrix $P_m \otimes Q_m$ does not need to be explicitly computed and stored. Indeed, letting $Z \in \mathbb{R}^{m \times m}$ be such that $z = \text{vec}(Z)$, it holds that $x_m^{\otimes} = \text{vec}(Q_m Z P_m^T)$; moreover, $(P_m \otimes Q_m)^T b = \text{vec}((Q_m^T b_1)(b_2^T P_m))$. The following proposition provides a cheaper computation in case both T_1 and T_2 are diagonalizable, as is the case for instance when they are both symmetric.

Proposition 3.1 *Assume that the matrices T_1, T_2 are diagonalizable, and let $T_1 = X\Lambda X^{-1}$, $T_2 = Y\Theta Y^{-1}$ be their eigendecompositions. Let*

$$g = f(\Theta \otimes I_m + I_m \otimes \Lambda)\text{vec}(X^{-1} Q_m^T b_1 b_2^T P_m Y^{-T}) \in \mathbb{R}^{m^2}.$$

With the notation and assumptions above, for G such that $g = \text{vec}(G)$ it holds that

$$x_m^{\otimes} = \text{vec}(Q_m X G Y^T P_m^T).$$

Proof Using the properties of the Kronecker product (see, e.g., [29, Corollary 4.2.11 and Theorem 4.4.5]), the eigendecomposition of $\mathcal{T}_m = T_2 \otimes I + I \otimes T_1$ is given by

$$T_2 \otimes I + I \otimes T_1 = (Y \otimes X)(\Theta \otimes I_m + I_m \otimes \Lambda)(Y^{-1} \otimes X^{-1}),$$

so that $f(\mathcal{T}_m) = (Y \otimes X) f(\Theta \otimes I_m + I_m \otimes \Lambda)(Y^{-1} \otimes X^{-1})$, where $f(\Theta \otimes I_m + I_m \otimes \Lambda)$ is a diagonal matrix. The result follows from explicitly writing down the eigenvector matrices associated with each Kronecker product; note that $f(\Theta \otimes I_m + I_m \otimes \Lambda)$ can be computed cheaply as both Θ and Λ are diagonal. □

In addition to providing a computational procedure for determining $x_m^{\otimes}$, Proposition 3.1 reveals that, in exact arithmetic, the true vector $x = f(\mathcal{A})b$ can be obtained using information from spaces of dimension at most $m = \max\{n_1, n_2\}$, whereas the standard approximation x_m may require a much larger dimension space. This fact is due to both the Kronecker form of $\mathcal{A}$ and the composition of b, as b corresponds to the

Table 1 Example 3.2 for $f(x) = \sqrt{x}$, $b_2 \neq b_1$

m	$\|f(\mathcal{A})b - x_m\|$	$\|f(\mathcal{A})b - x_m^{\otimes}\|$
5	1.4416e+00	9.6899e−01
10	5.2832e−01	2.7151e−01
15	2.2517e−01	8.4288e−02
20	9.9517e−02	1.8327e−02
25	4.0681e−02	8.5632e−03
30	1.5114e−02	2.7162e−03
35	9.0086e−03	5.3891e−04
40	6.3515e−03	1.9269e−04
45	3.5355e−03	1.9476e−05
50	1.7627e−03	6.4440e−13

Table 2 Example 3.2 for $f(x) = \sqrt{x}$, $b_2 = b_1$

m	$\|f(\mathcal{A})b - x_m\|$	$\|f(\mathcal{A})b - x_m^{\otimes}\|$
5	1.9371e+00	1.5903e+00
10	7.5344e−01	4.5636e−01
15	3.3417e−01	1.3538e−01
20	1.4240e−01	2.5706e−02
25	5.1205e−02	1.1719e−12
30	1.2671e−02	1.1034e−12
35	5.1316e−03	1.4357e−12
40	1.7854e−03	1.1186e−12
45	6.2249e−04	1.2297e−12
50	1.8720e−04	1.2975e−12

"vectorization" of the rank-one matrix $b_1 b_2^T$. The following examples illustrate this property, while more explicit formulas can be obtained for the exponential function, as we will describe in Sect. 4.

Example 3.2 We consider $f(x) = \sqrt{x}$ and $M_1 = M_2 = -\text{tridiag}(1, -2, 1) \in \mathbb{R}^{n\times n}$, $n = 50$, each corresponding to the (scaled) centered three-point discretization of the one-dimensional negative Laplace operator in (0,1). We first consider b_1 equal to the vector of all ones, and b_2 a vector of random values uniformly distributed in (0, 1); the results are shown in Table 1. We observe that convergence is faster, in terms of space dimension, for $x_m^{\otimes}$. Moreover, once subspaces of dimension $m = n = 50$ are reached, a rather accurate approximation is obtained with the structure-preserving approach, as the full eigenspace of M_1 is generated. We next consider the case of $b_2 = b_1$ (the vector of all ones) and report the numerical experiments in Table 2. Convergence is even faster in the structure preserving method, as apparently convergence is faster with b_1 than with the original b_2. No major difference is observed in the standard procedure (Tables 1, 2).

Example 3.3 Data for this example are taken from [14]. We consider the function $f(z) = (e^{s\sqrt{z}} - 1)/z$ with $s = 10^{-3}$, and $A = M \otimes I + I \otimes M$, where M is the $n \times n$

Table 3 Example 3.3, for $f(x) = (e^{s\sqrt{z}} - 1)/z$ with $s = 10^{-3}$, here $n = 50$

m	$\|f(\mathcal{A})b - x_m\|$	$\|f(\mathcal{A})b - x_m^{\otimes}\|$	$\frac{\|x_m - x_{m,old}\|}{\|x_m\|}$	$\frac{\|x_m^{\otimes} - x_{m,old}^{\otimes}\|}{\|x_m^{\otimes}\|}$
4	4.2422e−01	3.9723e−01	1.0000e+00	1.0000e+00
8	2.6959e−01	2.1025e−01	2.2710e−01	2.5313e−01
12	1.7072e−01	1.0365e−01	1.3066e−01	1.2971e−01
16	1.0324e−01	4.2407e−02	8.3444e−02	6.9960e−02
20	5.7342e−02	1.1176e−02	5.4224e−02	3.3969e−02
24	2.7550e−02	4.8230e−04	3.4054e−02	1.0935e−02
28	1.0351e−02	2.8883e−12	1.9296e−02	4.8230e−04
32	3.4273e−03	2.8496e−12	8.3585e−03	1.1366e−13
36	2.2906e−03	2.9006e−12	1.7514e−03	1.4799e−13
40	9.4368e−04	2.8119e−12	1.6283e−03	2.7323e−13
44	4.3935e−04	2.7593e−12	6.2797e−04	2.1786e−13
48	1.8744e−04	2.8235e−12	3.0332e−04	2.5965e−13

tridiagonal matrix of the finite difference discretization of the one-dimensional Laplace operator; $b := b_1 = b_2$ is the vector of all ones. Table 3 shows the approximation history of the standard method and of the new approach for $n = 50$. Because of the small size, we could compute and monitor the true error. In the last two columns, however, we also report the relative difference between the last two approximation iterates, which may be considered as a simple-minded error estimate to be used as stopping criterion for larger n; see, e.g., [13] or [31] for more sophisticated criteria. The results are as those of the previous examples. In Table 4 we report the runs for $n = 100$, for which we could not compute the exact solution, so that only the error estimates are reported. The results are very similar to the smaller case. In this case, memory requirements of the structured approximation become significantly lower than for the standard approach.

4 The case of the matrix exponential

The evaluation of (1.1) with $f(\mathcal{A}) = \exp(\mathcal{A})$ presents special interest owing to its importance in the numerical solution of time-dependent ODEs and PDEs [26–28]. The problem also arises in network science, when evaluating the *total communicability* of a network [6,12]. The exponential function provides a particularly favorable setting in the case of a matrix having Kronecker form. Indeed, due to the property (see, e.g., [25, Theorem 10.9]) $\exp(T_2 \otimes I_m + I_m \otimes T_1) = \exp(T_2) \otimes \exp(T_1)$, formula (3.1) simplifies even further. Indeed, we obtain

$$\begin{aligned} x_m^{\otimes} &= (P_m \otimes Q_m) \exp(T_2 \otimes I_m + I_m \otimes T_1)(P_m \otimes Q_m)^T b \\ &= (P_m \otimes Q_m)(\exp(T_2) \otimes \exp(T_1))(P_m \otimes Q_m)^T b \\ &= \mathrm{vec}(Q_m \exp(T_1) Q_m^T b_1 b_2^T P_m \exp(T_2)^T P_m^T) \\ &= \mathrm{vec}(x_m^{(1)} (x_m^{(2)})^T), \end{aligned} \tag{4.1}$$

Table 4 Example 3.3. For $f(x) = (e^{s\sqrt{z}} - 1)/z$ with $s = 10^{-3}$ and $b_2 = b_1$. Here $n = 100$

m	$\frac{\|x_m - x_{m,old}\|}{\|x_m\|}$	$\frac{\|x_m^{\otimes} - x_{m,old}^{\otimes}\|}{\|x_m^{\otimes}\|}$
4	1.0000e+00	1.0000e+00
8	2.3942e−01	2.7720e−01
12	1.5010e−01	1.6289e−01
16	1.0716e−01	1.0966e−01
20	8.1062e−02	7.8150e−02
24	6.3308e−02	5.7003e−02
28	5.0347e−02	4.1674e−02
32	4.0409e−02	2.9992e−02
36	3.2507e−02	2.0802e−02
40	2.6052e−02	1.3446e−02
44	2.0667e−02	7.5529e−03
48	1.6104e−02	2.9970e−03
52	1.2194e−02	3.1470e−04
56	8.8234e−03	1.1354e−12
60	5.9194e−03	3.4639e−13

with $x_m^{(1)} = Q_m \exp(T_1) Q_m^T b_1$ and $x_m^{(2)} = P_m \exp(T_2)(P_m^T b_2)$. The final approximation $x_m^{\otimes}$ is thus the simple combination of the two separate approximations of $\exp(M_1)b_1$ and $\exp(M_2)b_2$. Indeed, the same approximation could be obtained by first writing

$$\exp(\mathcal{A})b = \exp(M_2) \otimes \exp(M_1)b = \mathrm{vec}((\exp(M_1)b_1)(b_2^T \exp(M_2)^T), \quad (4.2)$$

and then using the standard approximations $\exp(M_1)b_1 \approx Q_m \exp(T_1) Q_m^T b_1$ and $\exp(M_2)b_2 \approx P_m \exp(T_2) P_m^T b_2$.

We next illustrate the approximation behavior to the matrix exponential with a few numerical examples, using the standard Krylov subspace.

We stress that because of the decreased memory allocations to generate $K_m(M_i, b_i)$, the computation of $x_m^{\otimes}$ can afford significantly larger values of m, than when building $K_m(\mathcal{A}, b)$.

Example 4.1 We consider the approximation of $\exp(\mathcal{A})b$ with $\mathcal{A}$ as in (1.2) and $M_1 = \mathrm{tridiag}(1, -2, 1)$ and $M_2 = \mathrm{tridiag}(2, -3, 2)$, both of size $n_1 = n_2 = 70$. Therefore, $\mathcal{A}$ has dimension 4900. Moreover, we take $b_1 = [1, \ldots, 1]^T$ and b_2 a vector with random values uniformly distributed in $(0, 1)$. Thanks to the problem size, the vector $\exp(\mathcal{A})b$ could be computed explicitly. Figure 1(left) reports the convergence history as the space dimension m increases when using two different approaches: the first one uses $K_m(\mathcal{A}, b)$ as approximation space, so that $x_m = \mathcal{V}_m \exp(H_m)(\mathcal{V}_m^T b)$ with $H_m = \mathcal{V}_m^T \mathcal{A} \mathcal{V}_m$; the second one uses $x_m^{\otimes}$ in (4.1). We observe that the convergence of $x_m^{\otimes}$ is faster than that of x_m; this fact will be explored in Sect. 4.1. The plot also reports the error norm in the approximation of $x^{(1)}$ and $x^{(2)}$: the error norm for $x_m^{\otimes}$ is mainly driven by that of the most slowly converging approximation between $x_m^{(1)}$ and $x_m^{(2)}$.

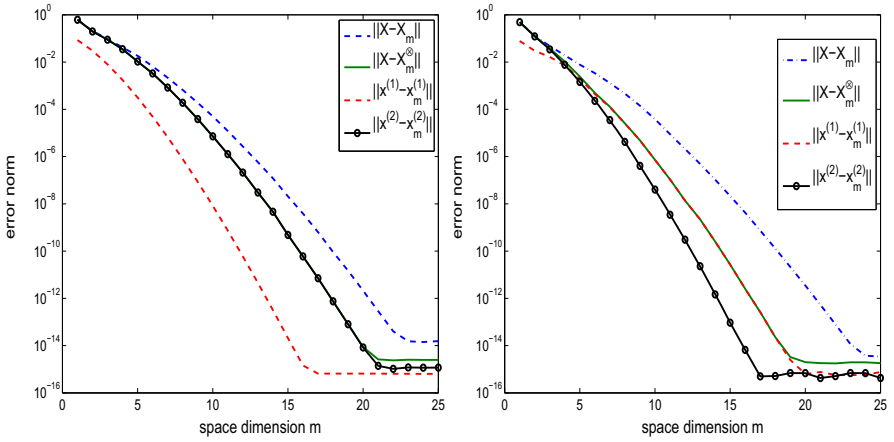

Fig. 1 Convergence history to $\exp(\mathcal{A})b$. *Left* Example 4.1. *Right* Example 4.2

Example 4.2 We modify Example 4.1 by setting $M_2 = \text{tridiag}(1, -2, 1)$, while M_1 to be equal to the discretization by finite differences of the one-dimensional non-selfadjoint operator $\mathcal{L}(u) = u_{xx} - 100u_x$ on the interval $[0, 1]$. Hence, M_1 (and therefore $\mathcal{A}$) is nonsymmetric. The matrix dimensions and the vectors b_1, b_2 are as in the previous example. The convergence history is reported in the right plot of Fig. 1. Similar comments as for Example 4.1 can be deduced.

Example 4.3 The next example arises in graph and network analysis. Given two graphs $G_1 = (V_1, E_1)$ and $G_2 = (V_2, E_2)$, we consider the Cartesian product $\mathcal{G} = G_1 \square G_2$ of the two given graphs, defined as follows. The vertex set of $\mathcal{G}$ is just the Cartesian product $V_1 \times V_2$, and there is an edge between two vertices (u_1, u_2) and (v_1, v_2) of $\mathcal{G}$ if either $u_1 = v_1$ and $(u_2, v_2) \in E_2$, or $u_2 = v_2$ and $(u_1, v_1) \in E_1$. The adjacency matrix of $\mathcal{G}$ is then the Kronecker sum of the adjacency matrices of G_1 and G_2 [1, page 37]; see also [42] for definitions (and applications) in the case of directed graphs. A useful notion in the analysis of complex networks is the *total communicability*, which is defined as the row sum of the exponential of the adjacency matrix, see [6]. The entries of this vector provide a measure of the "importance" of the nodes in the network, and can be computed as $\exp(\mathcal{A})b$ where now b is the vector of all ones (note that the corresponding matrix B has rank one). We consider five Cartesian product graphs of the form $\mathcal{G}_i = G_i \square G_i$, with each G_i being a Barabasi–Albert graph constructed using the preferential attachment model. The command `pref` in the Matlab toolbox CONTEST [40] was used (with the default choice of parameters) to generate five graphs on n nodes, where $n = 1000, 2000, \ldots, 5000$. Thus, the adjacency matrices of the corresponding Cartesian product graphs $\mathcal{G}_i$ have dimension ranging between one and twenty-five millions. All the resulting matrices are symmetric indefinite.

Table 5 reports the CPU time required to compute a basis for the Krylov subspace of dimension $m = 30$ as the graph matrix size increases (all runs were performed with Matlab R2011b [34] on a laptop with Intel Core i7-3687U CPU running at 2.10Ghz with 7.7GiB memory). The last column reports the time when $\mathcal{A}$ is used, so that

Table 5 Example 4.3. CPU Time for the construction of the Krylov approximation space of dimension $m = 30$ when using either $M_1 \in \mathbb{R}^{n\times n}$ (symmetric) or $\mathcal{A} = M_1 \otimes I + I \otimes M_1 \in \mathbb{R}^{n^2\times n^2}$. Only results for the smallest graph matrices $\mathcal{A}$ are reported when building $K_m(\mathcal{A}, b)$

n	CPU Time $K_m(M_1, b_1)$	CPU Time $K_m(\mathcal{A}, b)$
1000	0.02662	29.996
2000	0.04480	189.991
3000	0.06545	–
4000	0.90677	–
5000	0.99206	–

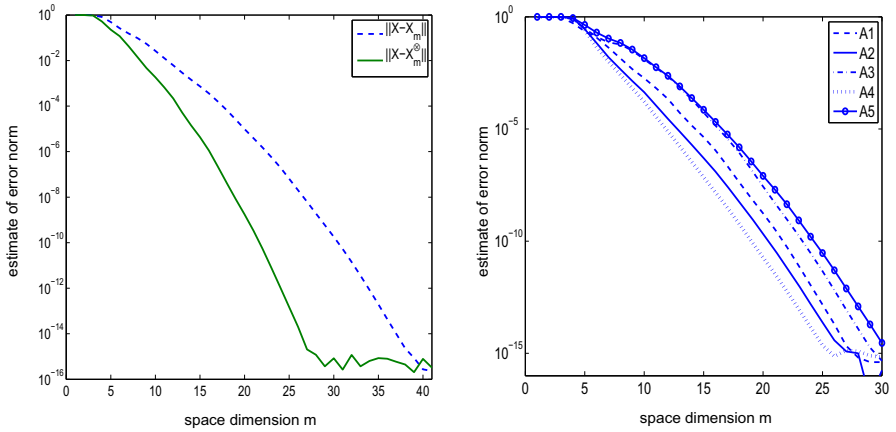

Fig. 2 Example 4.3. Convergence history to $\exp(\mathcal{A})b$. *Left* Example 4.3, case $n = 1000$. *Right* Example 4.3, convergence history for all five cases

$\mathcal{V}_m \exp(H_m)e_1\|b\|$ is computed; the middle column refers to the case when M_1 is used, so that $x_m^{\otimes}$ in (4.1) is computed. As expected, the CPU time for $K_m(M_1, b_1)$ is several orders of magnitude smaller than for $K_m(\mathcal{A}, b)$. In the latter case, timings became prohibitive for $n = 3{,}000$, since the generation of the basis for the space entails the orthogonalization of vectors in $\mathbb{R}^{n^2}$. The computational costs remain extremely low when computing a basis for $K_m(M_1, b_1)$. The left plot of Fig. 2 shows the convergence history of the two approaches, in terms of space dimensions, when the smallest matrix in the set is used. Convergence is monitored by measuring the difference between the last two iterates, as done in the previous examples. Once again, convergence is faster when the Kronecker form is exploited. The right plot of Fig. 2 reports the convergence history of $x_m^{\otimes}$ for all matrices in the set. All spectra are roughly contained in the interval $[-15, 15]$, therefore the expected convergence rate is approximately the same for all matrices.

Remark 4.4 Besides the exponential, the matrix sine and cosine are also well-behaved with respect to the Kronecker sum structure. Indeed, the identities $\sin(M_1 \oplus M_2) =$

$\sin(M_1)\otimes\cos(M_2)+\cos(M_1)\otimes\sin(M_2)$ and $\cos(M_1\oplus M_2)=\cos(M_1)\otimes\cos(M_2)-\sin(M_1)\otimes\sin(M_2)$ hold [25, Theorem 12.2], which can be exploited to greatly reduce the computational cost and storage requirements for the evaluation of $f(\mathcal{A})b$ when f is either the sine or cosine or a combination of these functions.

4.1 Convergence considerations

An expression for the error can be deduced by using the form in (4.2). Indeed, letting $x^{(1)}=\exp(M_1)b_1$ and $x^{(2)}=\exp(M_2)b_2$, and also $X=x^{(1)}(x^{(2)})^T$ and $X_m^{\otimes}=x_m^{(1)}(x_m^{(2)})^T$, it holds

$$\begin{aligned}\|\exp(\mathcal{A})b-x_m^{\otimes}\| &= \|X-X_m^{\otimes}\|_F\\ &= \|x^{(1)}(x^{(2)}-x_m^{(2)})^T+(x^{(1)}-x_m^{(1)})(x_m^{(2)})^T\|_F\\ &\le \|x^{(1)}\|\,\|x^{(2)}-x_m^{(2)}\|+\|x^{(1)}-x_m^{(1)}\|\,\|x_m^{(2)}\|. \end{aligned}\tag{4.3}$$

Therefore, the error norm in the approximation to $\exp(\mathcal{A})b$ is bounded by the errors of the two separate approximations with M_1 and M_2. The relation (4.3) can also be used for deriving a priori convergence bounds for $\exp(\mathcal{A})b$ in terms of the bounds for M_1 and M_2. We will give such bounds in the case M_1 and M_2 are Hermitian and positive definite. The following result was proved in [26].

Theorem 4.5 *Let M be a Hermitian positive semidefinite matrix with eigenvalues in the interval $[0,4\rho]$. Then the error in the Arnoldi approximation of $\exp(-\tau M)v$ with $\|v\|=1$, namely, $\varepsilon_m:=\|\exp(-\tau M)v-V_m\exp(-\tau T_m)e_1\|$, is bounded in the following ways:*

(i) $\varepsilon_m\le 10\exp(-m^2/(5\rho\tau))$, *for* $\rho\tau\ge 1$ *and* $\sqrt{4\rho\tau}\le m\le 2\rho\tau$;
(ii) $\varepsilon_m\le 10(\rho\tau)^{-1}\exp(-\rho\tau)\left(\frac{e\rho\tau}{m}\right)^m$ *for* $m\ge 2\rho\tau$.

We next show how Theorem 4.5 can be used to compare the difference in convergence rates between x_m and $x_m^{\otimes}$. To simplify the presentation, we assume that $M=M_1=M_2$, and that $b_1=b_2$, with $\|b_1\|=1$. We refer the reader to [5,30] for estimates similar to those of Theorem 4.5.

It can be shown that if λ_i, $i=1,\ldots,n$ are the eigenvalues of M (in decreasing order), then the n^2 eigenvalues of $\mathcal{A}$ are given by $\lambda_i+\lambda_j$, $i,j\in\{1,\ldots,n\}$; see, e.g., [29, Theorem 4.4.5]. Therefore in particular, the largest and smallest eigenvalues of $\mathcal{A}$ equal $2\lambda_1$ and $2\lambda_n$, respectively. If we apply Theorem 4.5 to $M-\lambda_n I$ for $\tau=1$, then we obtain that for m large enough the error is bounded as

$$\varepsilon_m(M)\le 10\frac{\exp(-\rho)}{\rho}\left(\frac{e\rho}{m}\right)^m,\quad \rho=\frac{\lambda_1-\lambda_n}{4}.$$

On the other hand, Theorem 4.5 applied to $\mathcal{A}-2\lambda_n I$ yields

$$\varepsilon_m(\mathcal{A})\le 10\frac{\exp(-\widehat{\rho})}{\widehat{\rho}}\left(\frac{e\widehat{\rho}}{m}\right)^m,\quad \widehat{\rho}=\frac{2\lambda_1-2\lambda_n}{4}=2\rho.$$

The ratio between the two bounds is given by

$$\frac{\exp\left(\frac{\rho}{2}\right)}{2^{m-1}},$$

which is in favor of the computation with M for small ρ. In case ρ is very large, both methods become very slow.

5 The case of the matrix inverse

Also very important in applications is the case of the inverse, $f(\mathcal{A}) = \mathcal{A}^{-1}$ where $\mathcal{A}$ has Kronecker sum structure. The solution of linear systems of the form $\mathcal{A}x = b$ arises in many applications (PDEs, imaging, Markov chains, networks, etc.) and Krylov subspace methods are widely used, typically together with preconditioning, to solve such systems. The Kronecker structure can be readily exploited if b is the result of the vectorization of a low rank matrix. For simplicity, let us assume that $b = \mathrm{vec}(b_1 b_2^T)$. Then the system $\mathcal{A}x = b$ is equivalent to the following Sylvester equation (see, e.g., [29, Sec. 4.4]):

$$M_1 X + X M_2^T = b_1 b_2^T, \quad x = \mathrm{vec}(X). \tag{5.1}$$

Numerical methods that exploit the small size of M_1, M_2 can be used to solve the linear matrix equation in (5.1). If n_1 and n_2 are of order up to a few thousands, then the Bartels–Stewart algorithm can be used [2]. Otherwise, X can be approximated by using different approaches, depending on the relative size of n_1 and n_2 [38]. Here we briefly describe the idea of approximate solution by projection onto an appropriate subspace, which will be used in Sect. 6.2. For simplicity of exposition we assume $M_2 = M_1$ and $b_2 = b_1$; if this is not the case, straightforward modifications can be included; see [38]. If the orthonormal columns of $P_m (= Q_m)$ are a basis for the considered subspace of $\mathbb{R}^n$ of dimension m, then an approximation to X is sought as $X \approx X_m = P_m Y_m P_m^T$, where $Y_m \in \mathbb{R}^{m\times m}$ is determined by imposing additional conditions. A common strategy consists of imposing that the residual $R_m := M_1 X_m + X_m M_1^T - b_1 b_1^T$ be orthogonal to the generated subspace, that is, $(P_m \otimes P_m)^T \mathrm{vec}(R_m) = 0$, or, in matrix terms, $P_m^T R_m P_m = 0$, where a zero matrix appears on the right-hand side. Substituting in this last equation the definition of R_m and X_m, gives

$$P_m^T M_1 P_m Y_m P_m^T P_m + P_m^T P_m Y_m P_m^T M_1^T P_m - P_m^T b_1 b_1^T P_m = 0.$$

Recalling that $P_m^T P_m = I$ and that $P_m^T M_1 P_m = T_1$, we obtain the small scale linear equation

$$T_1 Y_m + Y_m T_1^T - \widehat{b}_1 \widehat{b}_1 = 0, \quad \widehat{b}_1 = P_m^T b_1,$$

whose solution yields Y_m.

For later convenience, we notice that the approximate solution $x_m^{\otimes} = \mathrm{vec}(X_m)$ to $f(\mathcal{A})b = \mathcal{A}^{-1}b$ can be written in the more familiar form

$$x_m^{\otimes} = \mathrm{vec}(P_m Y_m P_m^T) = (P_m \otimes P_m)\mathrm{vec}(Y_m)$$
$$= (P_m \otimes P_m)(T_1 \otimes I + I \otimes T_1)^{-1}(P_m \otimes P_m)^T b. \tag{5.2}$$

6 Completely monotonic functions

Both the matrix exponential (in the form $f(\mathcal{A}) = \exp(-\mathcal{A})$) and the inverse are special cases of an important class of analytic functions, namely, the completely monotonic functions [41]. We recall the following definitions.

Definition 6.1 Let f be defined in the interval (a, b) where $-\infty \le a < b \le +\infty$. Then, f is said to be *completely monotonic* in (a, b) if

$$(-1)^k f^{(k)}(x) \ge 0 \quad \text{for all } a < x < b \quad \text{and all} \quad k = 0, 1, 2, \ldots$$

Moreover, f is said to be *strictly completely monotonic* in (a, b) if

$$(-1)^k f^{(k)}(x) > 0 \quad \text{for all } a < x < b \quad \text{and all} \quad k = 0, 1, 2, \ldots$$

Here $f^{(k)}$ denotes the kth derivative of f, with $f^{(0)} \equiv f$.

An important theorem of Bernstein states that a function f is completely monotonic in $(0, \infty)$ if and only if f is the Laplace–Stieltjes transform of $\alpha(\tau)$;

$$f(x) = \int_0^\infty e^{-\tau x}\, \mathrm{d}\alpha(\tau), \tag{6.1}$$

where $\alpha(\tau)$ is nondecreasing and the integral in (6.1) converges for all $x > 0$. See [41, Chapter 4]. For this reason, completely monotonic functions on $(0, \infty)$ are also referred to as *Laplace–Stieltjes functions*.

Important examples of Laplace–Stieltjes functions include:

1. $f_1(x) = 1/x = \int_0^\infty e^{-x\tau} d\alpha_1(\tau)$ for $x > 0$, where $\alpha_1(\tau) = \tau$ for $\tau \ge 0$.
2. $f_2(x) = e^{-x} = \int_0^\infty e^{-x\tau} d\alpha_2(\tau)$ for $x > 0$, where $\alpha_2(\tau) = 0$ for $0 \le \tau < 1$ and $\alpha_2(\tau) = 1$ for $\tau \ge 1$.
3. $f_3(x) = (1 - e^{-x})/x = \int_0^\infty \mathrm{e}^{-x\tau} d\alpha_3(\tau)$ for $x > 0$, where $\alpha_3(\tau) = \tau$ for $0 \le \tau \le 1$, and $\alpha_3(\tau) = 1$ for $\tau \ge 1$.

Also, the functions $x^{-\sigma}$ (for any $\sigma > 0$), $\log(1 + 1/x)$ and $\exp(1/x)$, are all strictly completely monotonic on $(0, \infty)$. Moreover, products and positive linear combinations of strictly completely monotonic functions are strictly completely monotonic.

Formula (6.1) suggests the use of quadrature rules to approximate $f(\mathcal{A})b$ when $\mathcal{A}$ is a Kronecker sum and f is strictly completely monotonic on $(0, \infty)$:

$$f(\mathcal{A})b = \int_0^\infty \exp(-\tau\mathcal{A})b\, \mathrm{d}\alpha(\tau) \approx \sum_{k=1}^{q} w_k \exp(-\tau_k \mathcal{A})b, \tag{6.2}$$

where $\tau_1, \ldots, \tau_k \in (0, \infty)$ are suitably chosen quadrature nodes and $w_1, \ldots, w_k \in \mathbb{R}$ are the quadrature weights; see, for example, [21, Sec. 5]. As shown in the previous section, the Kronecker sum structure can be exploited in the computation of the individual terms $\exp(-\tau_k \mathcal{A})b$. Also note that each contribution to the quadrature can be computed independently of the others, which could be useful in a parallel setting. This approach could be especially useful in cases where convergence of the Krylov subspace approximation is slow.

In the case of interpolatory quadrature and Hermitian matrices, the absolute error $\| f(\mathcal{A})b - \sum_{k=1}^{q} w_k \exp(-\tau_k \mathcal{A})b\|$ (in the 2-norm) is easily seen to be bounded by $\varepsilon \|b\|$, where ε is defined as

$$\varepsilon = \max_{i,j} \left| \int_0^\infty \exp(-\tau(\lambda_i + \mu_j))\, \mathrm{d}\alpha(\tau) - \sum_{k=1}^{q} w_k \exp(-\tau_k(\lambda_i + \mu_j)) \right|$$

and λ_i, μ_j range over the spectra of M_1, M_2, where $\mathcal{A} = M_2 \otimes I + I \otimes M_1$. In the case $M_1 = M_2 = M = M^*$, the error can be bounded by

$$\varepsilon \leq \max_{\lambda, \mu \in [\lambda_{\min}, \lambda_{\max}]} \left| \int_0^\infty \exp(-\tau(\lambda + \mu))\, \mathrm{d}\alpha(\tau) - \sum_{k=1}^{q} w_k \exp(-\tau_k(\lambda + \mu)) \right|,$$

where $\lambda_{\min}, \lambda_{\max}$ are the extreme eigenvalues of M. For additional discussion of error bounds associated with the use of quadrature rules of the form (6.2), see [21, Sec. 5.7].

Analogous considerations apply to more general types of functions. For a function f analytic inside a contour $\Gamma \in \mathbb{C}$ containing the eigenvalues of $\mathcal{A}$ in its interior and continuous on Γ we can write

$$f(\mathcal{A}) = \frac{1}{2\pi i} \int_\Gamma f(z)(\mathcal{A} - zI)^{-1}\, \mathrm{d}z.$$

Quadrature rules can be used to obtain approximations of the form

$$f(\mathcal{A})b = \frac{1}{2\pi i} \int_\Gamma f(z)(\mathcal{A} - zI)^{-1} b\, \mathrm{d}z \approx \sum_{k=1}^{q} w_k (\mathcal{A} - z_k I)^{-1} b,$$

requiring the solution of the q linear systems $(\mathcal{A} - z_k I)x = b$, possibly in parallel for $k = 1, \ldots, q$. We refer to [23] for details on how to apply this technique efficiently. Again, the Kronecker sum structure of $\mathcal{A}$, if present, can be exploited to greatly reduce the computational cost and storage requirements. In particular, if $b = \mathrm{vec}(b_1 b_2^T)$, then according to Sect. 5, each system $(\mathcal{A} - z_k I)x = b$ is equivalent to solving the linear matrix equation $(M_1 - z_k I)X + X M_2^T = b_1 b_2^T$, with $x = \mathrm{vec}(X)$.

Another important class of functions is given by the Cauchy–Stieltjes (or Markov-type) functions, which can be written as

$$f(z) = \int_\Gamma \frac{\mathrm{d}\gamma(\omega)}{z - \omega}, \quad z \in \mathbb{C} \backslash \Gamma,$$

where γ is a (complex) measure supported on a closed set $\Gamma \subset \mathbb{C}$ and the integral is absolutely convergent. This class is closely related to, but distinct from, the class of Laplace–Stieltjes functions; see [41, Chapter VIII] for a general treatment.

In this paper we are especially interested in the particular case $\Gamma = (-\infty, 0]$ so that

$$f(x) = \int_{-\infty}^{0} \frac{\mathrm{d}\gamma(\omega)}{x - \omega}, \quad x \in \mathbb{C}\backslash(-\infty, 0], \tag{6.3}$$

where γ is now a (possibly signed) real measure. Important examples of Cauchy–Stieltjes function that are frequently encountered in applications (see [20]) include

$$\begin{aligned} z^{-\frac{1}{2}} &= \int_{-\infty}^{0} \frac{1}{z-\omega} \frac{1}{\pi\sqrt{-\omega}} \mathrm{d}\omega, \\ \frac{e^{-t\sqrt{z}} - 1}{z} &= \int_{-\infty}^{0} \frac{1}{z-\omega} \frac{\sin(t\sqrt{-\omega})}{-\pi\omega} \mathrm{d}\omega, \\ \frac{\log(1+z)}{z} &= \int_{-\infty}^{-1} \frac{1}{z-\omega} \frac{1}{(-\omega)} \mathrm{d}\omega. \end{aligned}$$

6.1 Convergence analysis for Laplace–Stieltjes functions

For Laplace–Stieltjes functions and symmetric positive definite matrices, in this section we analyze the convergence rate of the approximation obtained by exploiting the Kronecker form.[2] Moreover, we compare this rate with that of the standard approximation with $\mathcal{A}$, and that of the approximation of M_1. We will mainly deal with standard Krylov approximations, as error estimates for the exponential are available. A few comments are also included for rational Krylov subspaces.

6.1.1 Analysis of Krylov subspace approximation

In this section we show that the convergence rate of the approximation when using $x_m^{\otimes}$ is higher than that with $x_m = \mathcal{V}_m f(H_m)\mathcal{V}_m^T b$. Moreover, it is also higher than the convergence rate of the approximation $x_m^{(1)}$ to $f(M_1)b_1$.

For simplicity of exposition we assume that $M_1 = M_2$ and $b_1 = b_2$, with $\|b_1\| = 1$.

Proposition 6.2 *Let f be a Laplace–Stieltjes function, and $x_m^{\otimes} = (P_m \otimes P_m) f(\mathcal{T}_m)(P_m \otimes P_m)^T b$ be the Kronecker approximation to $f(\mathcal{A})b$. Moreover, let $x^{(1)} = \exp(-\tau M_1)b_1$ and $x_m^{(1)} = P_m \exp(-\tau T_1) P_m^T b_1$.*

We also define the scaled quantity $\widehat{x}^{(1)} := e^{-\lambda_{\min}\tau} x^{(1)} = e^{-(M_1+\lambda_{\min} I)\tau} b_1$; analogously for $\widehat{x}_m^{(1)}$. Then

[2] The nonsymmetric case provides an extra challenge, as convergence of the low rank Kronecker form depends on the non-normality of the matrix A, but also on the regularity of the function f; see, e.g., [21, Prop. 5.9].

$$\|f(\mathcal{A})b - x_m^{\otimes}\| \le 2\int_0^\infty \|\widehat{x}^{(1)} - \widehat{x}_m^{(1)}\|\,\mathrm{d}\alpha(\tau).$$

Proof Recalling the notation of (4.1) and (4.2) leading to (4.3), we have

$$\begin{aligned}
\|f(\mathcal{A})b - x_m^{\otimes}\| &= \left\| \int_0^\infty (e^{-\tau\mathcal{A}}b - (P_m \otimes P_m)e^{-\tau\mathcal{T}_m}(P_m \otimes P_m)^T b)\mathrm{d}\alpha(\tau) \right\| \\
&\le \int_0^\infty (\|x^{(1)}\| + \|x_m^{(1)}\|)\,\|x^{(1)} - x_m^{(1)}\|\mathrm{d}\alpha(\tau) \\
&\le \int_0^\infty 2e^{-\lambda_{\min}\tau}\|x^{(1)} - x_m^{(1)}\|\mathrm{d}\alpha(\tau) \\
&= 2\int_0^\infty \|e^{-\tau(M_1+\lambda_{\min}I)}b_1 - P_m e^{-\tau(T_1+\lambda_{\min}I)}P_m^T b_1\|\,\mathrm{d}\alpha(\tau) \\
&= 2\int_0^\infty \|\widehat{x}^{(1)} - \widehat{x}_m^{(1)}\|\,\mathrm{d}\alpha(\tau),
\end{aligned}$$

where in the last inequality we have used $\lambda_{\min}(M_1) \le \lambda_{\min}(T_1)$, so that

$$\|x_m^{(1)}\| \le e^{-\lambda_{\min}(T_1)\tau} \le e^{-\lambda_{\min}(M_1)\tau}.$$

□

We remark that the extra shift in the matrix M_1 is what makes the solution $x_m^{\otimes}$ converge faster than $x_m^{(1)}$.

In light of Proposition 6.2, bounds for the error norm can be found by estimating the error norm in the approximation of the exponential function under the measure $\mathrm{d}\alpha$.

Depending on the function $\alpha(\tau)$, different approximation strategies need to be devised. Here we analyze the case $\mathrm{d}\alpha(\tau) = \frac{1}{\tau^\eta}d\tau$ for some $\eta \ge 0$; for instance, the function $f(x) = 1/\sqrt{x}$ falls in this setting with $\eta = 1/2$. Then

$$\|f(\mathcal{A})v - x_m^{\otimes}\| \le 2\int_0^\infty \frac{1}{\tau^\eta}\|\widehat{x}^{(1)} - \widehat{x}_m^{(1)}\|\mathrm{d}\tau.$$

The case $\eta = 0$ is special. Since $\tau^\eta = 1$, the integral on the right-hand side can be bounded as in [39, proof of (3.1)], so that it holds

$$\|f(\mathcal{A})v - x_m^{\otimes}\| \le 2\frac{\sqrt{\widehat{\kappa}}+1}{\lambda_{\min}\sqrt{\widehat{\kappa}}}\left(\frac{\sqrt{\widehat{\kappa}}-1}{\sqrt{\widehat{\kappa}}+1}\right)^m,$$

where $\widehat{\kappa} = (\lambda_{\max} + \lambda_{\min})/(\lambda_{\min} + \lambda_{\min})$.

We focus next on the case $\eta > 0$. We split the integral as

$$\int_0^\infty \frac{1}{\tau^\eta}\|\widehat{x}^{(1)} - \widehat{x}_m^{(1)}\|\mathrm{d}\tau = \int_0^{\frac{m^2}{4\rho}} \frac{1}{\tau^\eta}\|\widehat{x}^{(1)} - \widehat{x}_m^{(1)}\|\,\mathrm{d}\tau + \int_{\frac{m^2}{4\rho}}^\infty \frac{1}{\tau^\eta}\|\widehat{x}^{(1)} - \widehat{x}_m^{(1)}\|\,\mathrm{d}\tau =: I_1 + I_2. \tag{6.4}$$

Lemma 6.3 *With the previous notation, for $\eta > 0$ it holds*

$$I_2 \le \left(\frac{4\rho}{m^2}\right)^\eta \frac{\sqrt{\widehat{\kappa}}+1}{\lambda_{\min}\sqrt{\widehat{\kappa}}}\left(\frac{\sqrt{\widehat{\kappa}}-1}{\sqrt{\widehat{\kappa}}+1}\right)^m,$$

where $\widehat{\kappa} = (\lambda_{\max} + \lambda_{\min})/(\lambda_{\min} + \lambda_{\min})$.

Proof We note that in the given interval $\tau^\eta \ge \left(\frac{m^2}{4\rho}\right)^\eta$, so that

$$I_2 \le \left(\frac{4\rho}{m^2}\right)^\eta \int_{\frac{m^2}{4\rho}}^\infty \|\widehat{x}^{(1)} - \widehat{x}_m^{(1)}\|\,\mathrm{d}\tau \le \left(\frac{4\rho}{m^2}\right)^\eta \int_0^\infty \|\widehat{x}^{(1)} - \widehat{x}_m^{(1)}\|\,\mathrm{d}\tau.$$

Following [39, Prop. 3.1], an explicit bound for the last integral can be obtained, from which the bound follows. □

The derivation of an upper bound for I_1 in (6.4) is a little more involved.

Lemma 6.4 *With the previous notation, for $\eta > 0$ it holds*

$$I_1 \le 10\left(\frac{1}{\rho}\left(\frac{e\rho}{m}\right)^m \left(\frac{1}{2\lambda_{\min}+\rho}\right)^{m-\eta} \boldsymbol{\gamma}\left(m-\eta, \frac{2\lambda_{\min}+\rho}{2\rho}m\right) + \left(\frac{2\rho}{m}\right)^{\eta-\frac{1}{2}}\left(\frac{\pi}{2\lambda_{\min}}\right)^{\frac{1}{2}} e^{-2m\sqrt{\frac{2\lambda_{\min}}{5\rho}}}\right),$$

where $\boldsymbol{\gamma}$ is the lower incomplete Gamma function.

Proof We observe that the quantity $\|\widehat{x}^{(1)} - \widehat{x}_m^{(1)}\|$ in I_1 can be bounded by using Theorem 4.5 (see [26]), hence we further split I_1 as

$$I_1 = \int_0^{\frac{m}{2\rho}} \frac{1}{\tau^\eta}\|\widehat{x}^{(1)} - \widehat{x}_m^{(1)}\|\,\mathrm{d}\tau + \int_{\frac{m}{2\rho}}^{\frac{m^2}{4\rho}} \frac{1}{\tau^\eta}\|\widehat{x}^{(1)} - \widehat{x}_m^{(1)}\|\,\mathrm{d}\tau. \tag{6.5}$$

Theorem 4.5 can be applied to positive semidefinite matrices. Therefore we write $e^{-(M_1+\lambda_{\min}I)\tau} = e^{-2\lambda_{\min}\tau}e^{-(M_1-\lambda_{\min}I)\tau}$, with $M_1 - \lambda_{\min}I$ positive semidefinite. For the first integral in (6.5) we thus have [see Theorem 4.5(ii)]

$$
\begin{aligned}
&\int_0^{\frac{m}{2\rho}} \frac{1}{\tau^\eta} \|\widehat{x}^{(1)} - \widehat{x}_m^{(1)}\| \, \mathrm{d}\tau \\
&= \int_0^{\frac{m}{2\rho}} \frac{e^{-2\lambda_{\min}\tau}}{\tau^\eta} \|e^{-(M_1-\lambda_{\min} I)\tau} b - (P_m \otimes P_m) e^{-(\mathcal{T}_m - \lambda_{\min} I)\tau} \widehat{b}\| \, \mathrm{d}\tau \\
&\le 10 \int_0^{\frac{m}{2\rho}} \frac{e^{-(2\lambda_{\min}+\rho)\tau}}{\rho \tau^{\eta+1}} \left(\frac{e\rho\tau}{m}\right)^m \mathrm{d}\tau \\
&= 10 \frac{1}{\rho} \left(\frac{e\rho}{m}\right)^m \int_0^{\frac{m}{2\rho}} \tau^{m-\eta-1} e^{-(2\lambda_{\min}+\rho)\tau} \, \mathrm{d}\tau \\
&= 10 \frac{1}{\rho} \left(\frac{e\rho}{m}\right)^m \left(\frac{1}{2\lambda_{\min}+\rho}\right)^{m-\eta} \boldsymbol{\gamma}\left(m-\eta, \frac{2\lambda_{\min}+\rho}{2\rho} m\right).
\end{aligned}
$$

For the second integral in (6.5), after the same spectral transformation and also using $\frac{1}{\tau^\eta} \le \frac{1}{(m/(2\rho))^\eta}$ for $\tau \in [\frac{m}{2\rho}, \frac{m^2}{4\rho}]$, we obtain

$$
\begin{aligned}
\int_{\frac{m}{2\rho}}^{\frac{m^2}{4\rho}} \frac{1}{\tau^\eta} \|\widehat{x}^{(1)} - \widehat{x}_m^{(1)}\| \, \mathrm{d}\tau &\le 10 \int_{\frac{m}{2\rho}}^{\frac{m^2}{4\rho}} \frac{e^{-2\lambda_{\min}\tau}}{\tau^\eta} e^{-\frac{m^2}{5\rho\tau}} \, \mathrm{d}\tau \\
&\le 10 \left(\frac{2\rho}{m}\right)^{\eta-1/2} \int_{\frac{m}{2\rho}}^{\frac{m^2}{4\rho}} \frac{1}{\tau^{\frac{1}{2}}} e^{-2\lambda_{\min}\tau - \frac{m^2}{5\rho\tau}} \, \mathrm{d}\tau \\
&\le 10 \left(\frac{2\rho}{m}\right)^{\eta-1/2} \int_0^{\infty} \frac{1}{\tau^{\frac{1}{2}}} e^{-2\lambda_{\min}\tau - \frac{m^2}{5\rho\tau}} \mathrm{d}\tau.
\end{aligned}
$$

We then use [18, formula 3.471.15], namely $\int_0^\infty x^{-\frac{1}{2}} e^{-\beta_1 x - \frac{\beta_2}{x}} dx = \sqrt{\frac{\pi}{\beta_1}} e^{-2\sqrt{\beta_1\beta_2}}$, to finally write

$$
10 \left(\frac{2\rho}{m}\right)^{\eta-1/2} \int_0^{\infty} \frac{1}{\tau^{\frac{1}{2}}} e^{-2\lambda_{\min}\tau - \frac{m^2}{5\rho\tau}} \mathrm{d}\tau = 10 \left(\frac{2\rho}{m}\right)^{\eta-1/2} \sqrt{\frac{\pi}{2\lambda_{\min}}} e^{-2\sqrt{\frac{2\lambda_{\min} m^2}{5\rho}}}.
$$

□

By collecting all bounds we can prove a final upper bound for the error, and give its asymptotic convergence rate. To this end, we first need the following technical lemma, whose proof is given in the appendix.

Lemma 6.5 *For $0 < x \le \alpha n$ with $0 < \alpha < 1$ it holds that*

$$
\boldsymbol{\gamma}(n, x) \le \frac{1}{1-\alpha} \frac{x^n}{n} e^{-x}.
$$

Theorem 6.6 *For $\eta > 0$ and with the notation above, it holds that*

$$\begin{aligned}\|f(\mathcal{A})v - x_m^{\otimes}\| &\le 2(I_1 + I_2)\\ &\le 20\left(\frac{1}{\rho}\left(\frac{e\rho}{m}\right)^m \left(\frac{1}{2\lambda_{\min}+\rho}\right)^{m-\eta} \boldsymbol{\gamma}\left(m-\eta, \frac{2\lambda_{\min}+\rho}{2\rho}m\right)\right.\\ &\quad \left. + \left(\frac{2\rho}{m}\right)^{\eta-1/2}\sqrt{\frac{\pi}{2\lambda_{\min}}}\, e^{-2m\sqrt{\frac{2\lambda_{\min}}{5\rho}}}\right)\\ &\quad + 20\left(\frac{4\rho}{m^2}\right)^{\eta}\frac{\sqrt{\widehat{\kappa}}+1}{\lambda_{\min}\sqrt{\widehat{\kappa}}}\left(\frac{\sqrt{\widehat{\kappa}}-1}{\sqrt{\widehat{\kappa}}+1}\right)^m\\ &= \mathcal{O}\left(\exp\left(-\frac{2m}{\sqrt{\widehat{\kappa}}}\right)\right) \quad \text{for } m \text{ and } \widehat{\kappa} \text{ large enough.} \end{aligned} \tag{6.6}$$

Proof We only need to show that the term involving $\boldsymbol{\gamma}$ is asymptotically bounded above by $\mathcal{O}\left(\exp\left(-\frac{2m}{\sqrt{\widehat{\kappa}}}\right)\right)$ for m and $\widehat{\kappa}$ large. Simple calculations show that the second argument of $\boldsymbol{\gamma}$ satisfies $(2\lambda_{\min}+\rho)/(2\rho)m \le \alpha m$ with $\alpha < 1$ for $\lambda_{\max}/\lambda_{\min} > 9$; the larger this eigenvalue ratio, the smaller α, so that for a large ratio, the bound $(2\lambda_{\min}+\rho)/(2\rho)m \le \alpha(m-\eta)$ also holds. Hence, we can use Lemma 6.5 to write $\boldsymbol{\gamma}(n,x) \approx e^{-x}\frac{x^n}{n}$. Therefore,[3]

$$\begin{aligned}&\frac{10}{\rho}\left(\frac{e\rho}{m}\right)^m \left(\frac{1}{2\lambda_{\min}+\rho}\right)^{m-\eta} \boldsymbol{\gamma}\left(m-\eta, \frac{2\lambda_{\min}+\rho}{2\rho}m\right)\\ &\approx \frac{10}{\rho}\left(\frac{e\rho}{m}\right)^m \left(\frac{1}{2\lambda_{\min}+\rho}\right)^{m-\eta}\left(\frac{2\lambda_{\min}+\rho}{2\rho}m\right)^{m-\eta}\frac{1}{m-\eta}e^{-\frac{2\lambda_{\min}+\rho}{2\rho}m}\\ &= 10\frac{2^\eta\rho^\eta - 1}{m^\eta(m-\eta)}\left(\frac{e}{2}\right)^m e^{-\frac{2\lambda_{\min}+\rho}{2\rho}m} = 10\frac{2^{\eta\rho^{\eta-1}}m^\eta(m-\eta)}{e^{\frac{2\lambda_{\min}+(\ln 4-1)\rho}{2\rho}m}}.\end{aligned}$$

Writing down $\rho = \frac{1}{4}(\lambda_{\max}-\lambda_{\min})$, and after a few algebraic calculations we obtain

$$\begin{aligned}\frac{2\lambda_{\min}+(\ln 4-1)\rho}{2\rho} &= \frac{1}{2}\frac{(\ln 4-1)\lambda_{\max}+(8-(\ln 4-1))\lambda_{\min}}{\lambda_{\max}-\lambda_{\min}}\\ &= \frac{1}{2}\left(\frac{4}{\widehat{\kappa}-1}+(\ln 4-1)\right) \ge \frac{2}{\sqrt{\widehat{\kappa}}},\end{aligned}$$

where the last inequality holds for $\widehat{\kappa}$ large enough (namely for $\widehat{\kappa} \ge 10$). □

The theorem above states that the convergence rate of the approximation depends on the condition number of the shifted matrix.

[3] We assume here that $m-\eta$ is a positive integer, otherwise we can take the Gamma function associated with the closest integer larger than $m-\eta$.

Remark 6.7 If $f(\mathcal{A})b$ is approximated in the Krylov subspace $K_m(\mathcal{A}, b)$, then the error norm can be written as

$$\|f(\mathcal{A})b - x_m\| \leq \int_0^\infty \|e^{-\tau\mathcal{A}}b - \mathcal{V}_m e^{-\tau H_m}\mathcal{V}_m^T b\| \mathrm{d}\alpha(\tau).$$

Therefore, all the previous steps can be replicated, leading to an estimate of the type

$$\|f(\mathcal{A})b - x_m\| \approx \exp\left(-\frac{2m}{\sqrt{\kappa}}\right) \tag{6.7}$$

where now $\kappa = \lambda_{\max}/\lambda_{\min}$. The improvement in the convergence rate when exploiting the Kronecker form thus becomes readily apparent, with the shift acting as an "accelerator". It is also important to realize that the error norm $\|f(M_1)b_1 - x_m^{(1)}\|$ is also driven by the same quantity κ as in (6.7), since the condition number of M_1 and $\mathcal{A}$ is the same. Therefore, it is really by using the Kronecker form that convergence becomes faster.

We next illustrate our findings with a simple example. A diagonal matrix is considered so as to be able to compute exact quantities, while capturing the linear convergence of the approximation.

Example We consider $f(x) = 1/\sqrt{x}$ (so that $\eta = 1/2$) and a diagonal matrix M_1 of size $n = 500$ with logarithmically distributed eigenvalues in $[10, 10^3]$, giving $\rho \approx 247$; b_1 is the vector of all ones, normalized to have unit norm. We wish to approximate $f(\mathcal{A})b$, with $b = \mathrm{vec}(b_1 b_1^T)$. We compare (see Fig. 3) the convergence curves of the usual approximation $x_m = \mathcal{V}_m f(H_m)e_1$ (solid thin line), with that of $x_m^{\otimes} = (Q_m \otimes Q_m) f(\mathcal{T}_m)\widehat{b}$ (dashed thick line). As expected, the convergence rate of the latter is better than for the standard method. The estimate in (6.6) is reported as thick crosses, and it well approximates the correct convergence slope. For completeness we also report the error norm $\|f(M_1)b_1 - Q_m f(T_1) Q_m^T b_1\|$, which behaves like that of the standard method, as noticed in the previous remark.

6.1.2 Rational Krylov subspace approximation

Convergence bounds of Laplace–Stieltjes functions are harder to obtain when rational Krylov subspaces are used, for few results on error bounds for the exponential function are available. In this section we discuss some of the results that can be obtained. However, we will show that additional results can be derived for the subclass of Cauchy–Stieltjes functions, since they involve inverses in place of exponential functions.

If the approximation space is the extended Krylov subspace, which can be defined as $K_m(M_1, b_1) + K_m(M_1^{-1}, M_1^{-1}b_1)$, error bounds are difficult to obtain for Laplace–Stieltjes functions, unless $\mathrm{d}\alpha = \mathrm{d}\tau$ (that is, $\eta = 0$). Indeed, for $\eta = 0$, we have

$$f(\mathcal{A})b - x_m^{\otimes} = \mathrm{vec}\left(\int_0^\infty \left(\exp(-\tau M_1)b_1 b_1^T \exp(-\tau M_1) - P_m \exp(-\tau\mathcal{T}_m)\widehat{b}_1\widehat{b}_1^T \exp(-\tau\mathcal{T}_m)P_m^T\right)\mathrm{d}\tau\right).$$

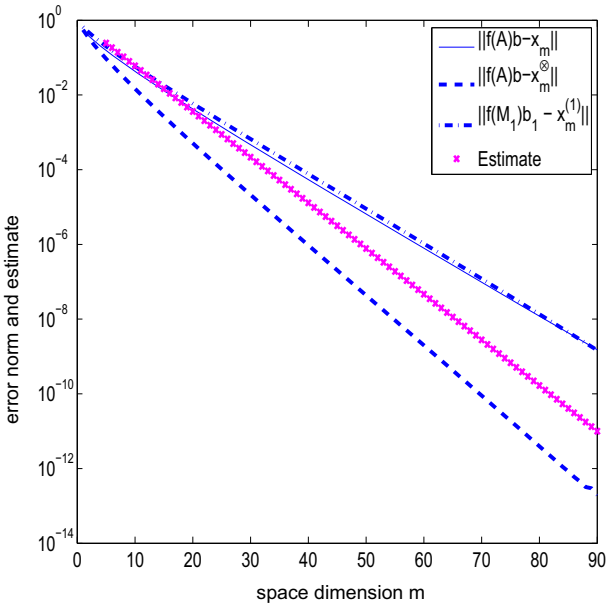

Fig. 3 Convergence curves for various approximation methods, and estimate in (6.6)

The integral coincides with the error matrix in the approximation of the numerical solution to the Lyapunov equation in the space Range(P_m).

This connection was already used in Lemma 6.3 to establish an upper bound for the Krylov subspace approximation. Here, we just mention that an asymptotic bound can be obtained by using results in [3,32,33], giving

$$\| f(\mathcal{A})b - x_m^{\otimes} \| \approx \mathcal{O}\left(\left(\frac{\sqrt[4]{\kappa} - 1}{\sqrt[4]{\kappa} + 1} \right)^m \right),$$

where $\kappa = \lambda_{\max}(\mathcal{A})/\lambda_{\min}(\mathcal{A}) = \lambda_{\max}(M_1)/\lambda_{\min}(M_1)$. Note that while there is no beneficial shifted matrix in this bound, the fourth root of κ appears, ensuring significantly faster convergence rate than for standard Krylov subspaces.

For $\eta > 0$, lack of explicit error bounds for the exponential function leaves the derivation of bounds for our setting an open problem. Nonetheless, experimental evidence seems to suggest a convergence rate similar to the one for $\eta = 0$.

Upper bounds for the exponential function when rational Krylov subspaces (2.2) are employed are usually asymptotic and specialized to optimal values of the parameters $\sigma_1, \ldots, \sigma_{m-1}$. We refer the reader to [20, sec. 4.2] for more details.

6.2 Convergence analysis for Cauchy–Stieltjes functions

Functions belonging to the Cauchy–Stieltjes class provide a more favorable setting, as they are based on the resolvent function. Assume then that f is a Cauchy–Stieltjes function. Using the definition in (6.3) and assuming that $b = \mathrm{vec}(b_1 b_1^T)$, we can write

$$
\begin{aligned}
f(\mathcal{A})b - x_m^{\otimes} &= f(\mathcal{A})b - (P_m \otimes P_m) f(\mathcal{T}_m)(P_m \otimes P_m)^T b \\
&= \int_{-\infty}^{0} (\mathcal{A} - \omega I)^{-1} b \, \mathrm{d}\gamma(\omega) - (P_m \otimes P_m) \int_{-\infty}^{0} (\mathcal{T}_m - \omega I)^{-1} (P_m \otimes P_m)^T b \, \mathrm{d}\gamma(\omega) \\
&= \int_{-\infty}^{0} \left((\mathcal{A} - \omega I)^{-1} b - (P_m \otimes P_m)(\mathcal{T}_m - \omega I)^{-1} (P_m \otimes P_m)^T b \right) \mathrm{d}\gamma(\omega).
\end{aligned}
$$

Let $M(\omega) = M_1 - \frac{\omega}{2} I$, so that for any v and V such that $v = \mathrm{vec}(V)$ we can write $(\mathcal{T}_m - \omega I)v = \mathrm{vec}(M(\omega)V + VM(\omega)^T)$. Then, recalling the derivation in (5.2), we obtain

$$
f(\mathcal{A})b - x_m^{\otimes} = \int_{-\infty}^{0} \mathrm{vec}(X(\omega) - X_m(\omega)) \mathrm{d}\gamma(\omega),
$$

where $X(\omega)$ and $X_m(\omega)$ are the exact and approximate solutions to the linear matrix equation $M(\omega)X + XM(\omega)^T = b_1 b_1^T$ when the space $K_m(M_1 - \frac{\omega}{2} I, b_1)$ is used. Note that this space is invariant under shift, that is $K_m(M_1, b_1) = K_m(M_1 - \omega I, b_1)$, so that the columns of P_m are still a basis for this space. An upper bound for the error can then be obtained as

$$
\| f(\mathcal{A})b - x_m^{\otimes} \| \le \int_{-\infty}^{0} \| X(\omega) - X_m(\omega) \|_F \mathrm{d}\gamma(\omega).
$$

Available convergence bounds for the approximation of $X(\omega)$ onto standard and rational Krylov subspaces can be employed as a first step towards an upper bound for the error norm above. Final bounds will then be obtained for specific choices of f, which yield specific functions $\gamma(\omega)$.

For standard Krylov subspaces, we can once again use [39, Proposition 3.1] to get

$$
\| f(\mathcal{A})b - x_m^{\otimes} \| \le \int_{-\infty}^{0} 2 \frac{\sqrt{\widehat{\kappa}_\omega} + 1}{(\lambda_{\min} - \frac{1}{2}\omega)\sqrt{\widehat{\kappa}_\omega}} \left(\frac{\sqrt{\widehat{\kappa}_\omega} - 1}{\sqrt{\widehat{\kappa}_\omega} + 1} \right)^m \mathrm{d}\gamma(\omega),
$$

where $\widehat{\kappa}_\omega = (\lambda_{\max} + \lambda_{\min} - \frac{1}{2}\omega)/(\lambda_{\min} + \lambda_{\min} - \frac{1}{2}\omega)$. For consistency with the previous notation, we shall use $\widehat{\kappa}_0 = \widehat{\kappa}$. Therefore,

$$
\| f(\mathcal{A})b - x_m^{\otimes} \| \le 2 \left(\frac{\sqrt{\widehat{\kappa}} - 1}{\sqrt{\widehat{\kappa}} + 1} \right)^m \int_{-\infty}^{0} \frac{\sqrt{\widehat{\kappa}_\omega} + 1}{(\lambda_{\min} - \frac{1}{2}\omega)\sqrt{\widehat{\kappa}_\omega}} \mathrm{d}\gamma(\omega), \tag{6.8}
$$

where $\left(\frac{\sqrt{\widehat{\kappa}} - 1}{\sqrt{\widehat{\kappa}} + 1} \right)^m \approx \exp(-2m/\sqrt{\widehat{\kappa}})$ for $\sqrt{\widehat{\kappa}}$ large. The final upper bound can be obtained once the measure $\mathrm{d}\gamma(\omega)$ is made more explicit, and this may influence the integration interval as well. For instance, for $f(x) = x^{-\frac{1}{2}}$,

$$
\int_{-\infty}^{0} \frac{\sqrt{\widehat{\kappa}_\omega} + 1}{(\lambda_{\min} - \frac{1}{2}\omega)\sqrt{\widehat{\kappa}_\omega}} \mathrm{d}\gamma(\omega)
$$

$$
\begin{aligned}
&= \int_{-\infty}^{0} \frac{\sqrt{\widehat{\kappa}_\omega}+1}{(\lambda_{\min}-\frac{1}{2}\omega)\sqrt{\widehat{\kappa}_\omega}} \frac{1}{\sqrt{-\omega}} \mathrm{d}\omega \\
&\leq 2\int_{-\infty}^{0} \frac{1}{(\lambda_{\min}-\frac{1}{2}\omega)} \frac{1}{\sqrt{-\omega}} \mathrm{d}\omega \\
&= 2\int_{-\infty}^{-1} \frac{1}{(\lambda_{\min}-\frac{1}{2}\omega)} \frac{1}{\sqrt{-\omega}} \mathrm{d}\omega + 2\int_{-1}^{0} \frac{1}{(\lambda_{\min}-\frac{1}{2}\omega)} \frac{1}{\sqrt{-\omega}} \mathrm{d}\omega \\
&\leq \int_{-\infty}^{-1} \frac{1}{(-\omega)} \frac{1}{\sqrt{-\omega}} \mathrm{d}\omega + 2\frac{1}{\lambda_{\min}} \int_{-1}^{0} \frac{1}{\sqrt{-\omega}} \mathrm{d}\omega = 2 + \frac{4}{\lambda_{\min}}.
\end{aligned}
$$

Since the inverse square root is both a Laplace–Stieltjes function and a Cauchy–Stieltjes function, it is not surprising that we get a similar convergence rate. The setting of this section allows one to determine a simpler expression for the bound.

Following similar steps as for the inverse square root, for $f(x) = \ln(1+x)/x$ we have (note the change in the integration interval)

$$
\begin{aligned}
\int_{-\infty}^{-1} \frac{\sqrt{\widehat{\kappa}_\omega}+1}{(\lambda_{\min}-\frac{1}{2}\omega)\sqrt{\widehat{\kappa}_\omega}} \mathrm{d}\gamma(\omega) &= \int_{-\infty}^{-1} \frac{\sqrt{\widehat{\kappa}_\omega}+1}{(\lambda_{\min}-\frac{1}{2}\omega)\sqrt{\widehat{\kappa}_\omega}} \frac{1}{-\omega} \mathrm{d}\omega \\
&\leq 2\int_{-\infty}^{-1} \frac{1}{(\lambda_{\min}-\frac{1}{2}\omega)} \frac{1}{(-\omega)} \mathrm{d}\omega \leq 2 \cdot 2 = 4.
\end{aligned}
$$

In both cases, the integral appearing in (6.8) is bounded by a constant of modest size, unless $\lambda_{\min}$ is tiny in the inverse square root. Summarizing, when using standard Krylov subspace approximation, $\|f(\mathcal{A})b - x_m^{\otimes}\|$ is bounded by a quantity whose asymptotic term is $\left(\frac{\sqrt{\widehat{\kappa}}-1}{\sqrt{\widehat{\kappa}}+1}\right)^m$ as m grows.

When using the extended Krylov subspace for an Hermitian positive definite M, this quantity is replaced by $\left(\frac{\sqrt[4]{\kappa}-1}{\sqrt[4]{\kappa}+1}\right)^m$, where m is the subspace dimension and $\kappa = \lambda_{\max}/\lambda_{\min}$ (see, e.g., [31], [33]), as conjectured in the case of Laplace–Stieltjes functions. Here, an explicit upper bound can actually be obtained.

Rational Krylov subspaces can also be used, and the term $\|X - X_m^{\otimes}\|_F$ can be estimated using, e.g., [9, Theorem 4.9].

7 Conclusions

In this paper we have shown how to take advantage of the Kronecker sum structure in $\mathcal{A}$ when using Krylov subspace methods to evaluate expressions of the form $f(\mathcal{A})b$. Special attention has been devoted to the important case of the matrix exponential. Numerical experiments demonstrate that considerable savings can be obtained when the Kronecker sum structure is exploited. A detailed analysis of the convergence rate of the new approximation for symmetric (or Hermitian) and positive definite matrices was also proposed.

Finally, while we have limited our presentation to the case where $\mathcal{A}$ is the Kronecker sum of two matrices, the same observations and techniques apply to the more general case where $\mathcal{A}$ is the Kronecker sum of three or more summands, since this can be reduced to the Kronecker sum of two matrices. For instance, if

$$\mathcal{A} = M_1 \oplus M_2 \oplus M_3 := M_1 \otimes I \otimes I + I \otimes M_2 \otimes I + I \otimes I \otimes M_3,$$

we can write

$$\mathcal{A} = M_1 \otimes (I \otimes I) + I \otimes (M_2 \otimes I + I \otimes M_3) =: M_1 \otimes I + I \otimes \mathcal{M},$$

and apply the techniques in this paper in a recursive fashion. Alternatively, one could use a fully tensorized approach, similar to those employed for generalized Sylvester equations in [33].

A challenging problem that has not been addressed here is the extension to the case of multi-term Kronecker sum, where $\mathcal{A} = \sum_{i=1}^{\ell} M_i \otimes G_i$, with general matrices M_i, G_i. Except for the function $f(z) = 1/z$—corresponding to the Sylvester equation for which projection methods have shown to be very well suited—even the two term problem ($\ell = 2$) provides a serious challenge.

Acknowledgements The authors would like to thank Paola Boito for her careful reading of the manuscript and helpful comments and two anonymous reviewers for their constructive criticism.

Appendix

In this appendix we prove Lemma 6.5.

Lemma 6.5. *For* $0 < x \le \alpha n$ *with* $0 < \alpha < 1$ *it holds that*

$$\boldsymbol{\gamma}(n, x) \le \frac{1}{1-\alpha} \frac{x^n}{n} e^{-x}.$$

Proof We have

$$\begin{aligned}
\boldsymbol{\gamma}(n, x) &= (n-1)! e^{-x} \left(e^x - \sum_{k=0}^{n-1} \frac{x^k}{k!} \right) = (n-1)! e^{-x} \left(\sum_{k=n}^{\infty} \frac{x^k}{k!} \right) \\
&= (n-1)! e^{-x} \frac{x^n}{n!} \left(1 + \sum_{j=1}^{\infty} \frac{x^j}{(n+1)\cdots(n+j)} \right) \\
&\le e^{-x} \frac{x^n}{n} \left(1 + \sum_{j=1}^{\infty} \alpha^j \frac{n^j}{(n+1)\cdots(n+j)} \right) \\
&\le e^{-x} \frac{x^n}{n} \left(\sum_{j=0}^{\infty} \alpha^j \right) = e^{-x} \frac{x^n}{n} \frac{1}{1-\alpha}.
\end{aligned}$$

□

References

1. Bapat, R.B.: Graphs and Matrices, Universitext, Springer. London; Hindustan Book Agency, New Dehli (2010)
2. Bartels, R.H., Stewart, G.W.: Algorithm 432: solution of the matrix equation $AX + XB = C$. Comm. ACM **15**(9), 820–826 (1972)
3. Beckermann, B.: An error analysis for rational Galerkin projection applied to the Sylvester equation. SIAM J. Numer. Anal. **49**(6), 2430–2450 (2011)
4. Beckermann, B., Kressner, D., Tobler, C.: An error analysis of Galerkin projection methods for linear systems with tensor product structure, SIAM J. Numer. Anal. **51**, 3307–3326 (2013)
5. Beckermann, B., Reichel, L.: Error estimation and evaluation of matrix functions via the Faber transform. SIAM J. Numer. Anal. **47**(5), 3849–3883 (2009)
6. Benzi, M., Klymko, C.: Total communicability as a centrality measure. J. Complex Netw. **1**(2), 124–149 (2013)
7. Benzi, M., Simoncini, V.: Decay bounds for functions of matrices with banded or Kronecker structure. SIAM J. Matrix Anal. Appl. **36–3**, 1263–1282 (2015)
8. Druskin, V., Knizhnerman, L.: Extended Krylov subspaces: approximation of the matrix square root and related functions. SIAM J. Matrix Anal. Appl. **19**, 755–771 (1998)
9. Druskin, V., Knizhnerman, L., Simoncini, V.: Analysis of the rational Krylov subspace and ADI methods for solving the Lyapunov equation. SIAM J. Numer. Anal. **49**, 1875–1898 (2011)
10. Druskin, V., Knizhnerman, L., Zaslavsky, M.: Solution of large scale evolutionary problems using rational Krylov subspaces with optimized shifts. SIAM J. Sci. Comput. **31**, 3760–3780 (2009)
11. Eiermann, M., Ernst, O.: A restarted Krylov subspace method for the evaluation of matrix functions. SIAM J. Numer. Anal. **44**, 2481–2504 (2006)
12. Estrada, E., Hatano, N., Benzi, M.: The physics of communicability in complex networks. Phys. Rep. **514**, 89–119 (2012)
13. Frommer, A., Güttel, S., Schweitzer, M.: Convergence of restarted Krylov subspace methods for Stieltjes functions of matrices. SIAM J. Matrix Anal. Appl **35**, 1602–1624 (2014)
14. Frommer, A., Güttel, S., Schweitzer, M.: Efficient and stable Arnoldi restarts for matrix functions based on quadrature. SIAM J. Matrix Anal. Appl. **35**, 661–683 (2014)
15. Frommer, A., Simoncini, V.: Matrix functions. In: Schilders, W.H.A., van der Vorst, H.A., Rommes, J. (eds.) Model Order Reduction: Theory, Research Aspects and Applications. Springer, Heidelberg (2008). (Mathematics in Industry)
16. Gavrilyuk, I.P., Hackbusch, W., Khoromskij, B.N.: $\mathscr{H}$-Matrix approximation for the operator exponential with applications. Numer. Math. **92**, 83–111 (2002)
17. Gavrilyuk, I.P., Hackbusch, W., Khoromskij, B.N.: Tensor-product approximation to the inverse and related operators in high-dimensional elliptic problems. Computing **74**, 131–157 (2005)
18. Gradshteyn, I.S., Ryzhik, I.M.: Table of Integrals, Series, and Products, 7th edn. Academic Press, New York (2007)
19. Grasedyck, L.: Existence and computation of low-rank approximations for large systems of tensor product structure. Computing **72**, 247–265 (2004)
20. Güttel, S.: Rational Krylov approximation of matrix functions: numerical methods and optimal pole selection. GAMM Mitt. **36**, 8–31 (2013)
21. Hackbusch, W.: Numerical tensor calculus. Acta Numer. **23**, 651–742 (2014)
22. Hackbusch, W., Khoromskij, B.N.: Low-rank Kronecker-product approximation to multi-dimensional nonlocal operators. II: HKT representation of certain operators. Computing **76**, 203–225 (2006)
23. Hale, N., Higham, N.J., Trefethen, L.N.: Computing A^{α}, $\log(A)$, and related matrix functions by contour integrals. SIAM J. Numer. Anal. **46**, 2505–2523 (2008)
24. Hansen, P.C., Nagy, J.G., O'Leary, D.P.: Deblurring Images: Matrices, Spectra, and Filtering. Society for Industrial and Applied Mathematics, Philadelphia (2006)
25. Higham, N.J.: Functions of Matrices—Theory and Computation. SIAM, Philadelphia (2008)
26. Hochbruck, M., Lubich, C.: On Krylov subspace approximations to the matrix exponential operator. SIAM J. Numer. Anal. **34**, 1911–1925 (1997)
27. Hochbruck, M., Lubich, C.: Exponential integrators for quantum-classical molecular dynamics. BIT Numer. Math. **39**, 620–645 (1999)
28. Hochbruck, M., Ostermann, A.: Exponential integrators. Acta Numer. **19**, 209–286 (2010)
29. Horn, R.A., Johnson, C.R.: Topics in Matrix Analysis. Cambridge University Press, Cambridge (1991)

30. Knizhnerman, L.: Calculus of functions of unsymmetric matrices using Arnoldi's method. Comput. Math. Math. Phys. **31**, 1–9 (1991)
31. Knizhnerman, L., Simoncini, V.: A new investigation of the extended Krylov subspace method for matrix function evaluations. Numer. Linear Algebra Appl. **17**, 615–638 (2010)
32. Knizhnerman, L., Simoncini, V.: Convergence analysis of the Extended Krylov Subspace Method for the Lyapunov equation. Numer. Math. **118**(3), 567–586 (2011)
33. Kressner, D., Tobler, C.: Krylov subspace methods for linear systems with tensor product structure. SIAM J. Matrix Anal. Appl. **31**(4), 1688–1714 (2010)
34. The MathWorks. Matlab 7.0. The Mathworks, Inc., Natick, MA (2014)
35. Moler, C., Van Loan, C.: Nineteen dubious ways to compute the exponential of a matrix, twenty-five years later. SIAM Rev. **45**, 3–49 (2003)
36. Ng, M.K.: Iterative Methods for Toeplitz Systems. Oxford University Press, Oxford (2004)
37. Palitta, D., Simoncini, V., Matrix-equation-based strategies for convection-diffusion equations. pp. 1–19 (2015) doi:10.1007/s10543-015-0575-8 (**to appear in BIT Numer. Math.**)
38. V. Simoncini, Computational Methods for Linear Matrix Equations, Technical report, Alma Mater Studiorum—Università di Bologna (2013) (**to appear in SIAM Review**)
39. Simoncini, V., Druskin, V.: Convergence analysis of projection methods for the numerical solution of large Lyapunov equations. SIAM J. Numer. Anal. **47**(2), 828–843 (2009)
40. Taylor, A., Higham, D.J.: CONTEST: A Controllable Test Matrix Toolbox for MATLAB. ACM Trans. Math. Softw. **35**, 26:1–26:17 (2009)
41. Widder, D.V.: The Laplace Transform. Princeton University Press, Princeton (1946)
42. Yang, C., Xu, J.-M.: Reliability of interconnection networks modeled by Cartesian product digraphs. Networks **52**, 202–205 (2008)